Supplementary Figure S1

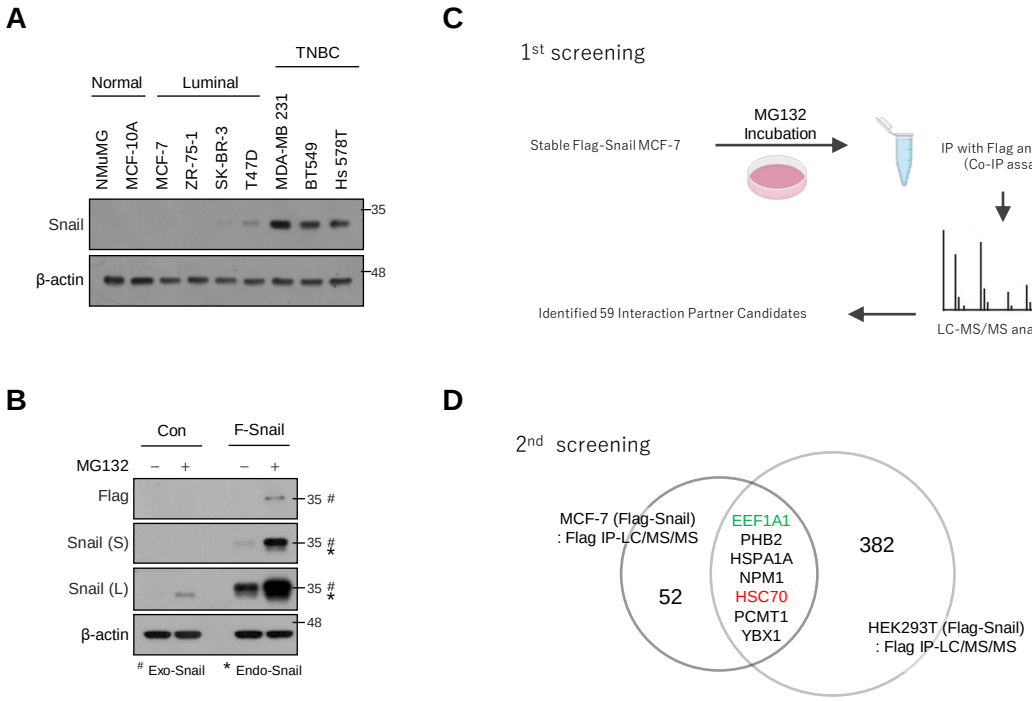

Fig. S1. Screening of Snail-interacting proteins. (**A**) Expression levels of Snail in normal breast cell lines, luminal-type, and triple-negative breast cancer cell lines. (**B**) Suppression of the proteasome pathway stabilizes Snail in Flag-Snail-expressing MCF-7 cells. MCF-7 cells were stably transfected with control and a Flag-tagged Snail-expressing vector, respectively. Snail-expressing MCF-7 cells were treated with 10 μM MG132 for 6 h and analyzed by western blotting with an anti-Flag or anti-Snail antibody. #: exogenously expressed Snail, *: endogenously expressed Snail. S: short exposure, L: long exposure. (**C**) Schematic for the screening of Snail-interacting proteins in MG132-treated Snail-expressing MCF-7 cells. (**D**) Venn diagram of Snail-interacting proteins in MCF-7 and HEK293T cells. The intersection depicts seven proteins that commonly interact with Snail in MCF-7 and HEK293T cells.

Supplementary Figure S2

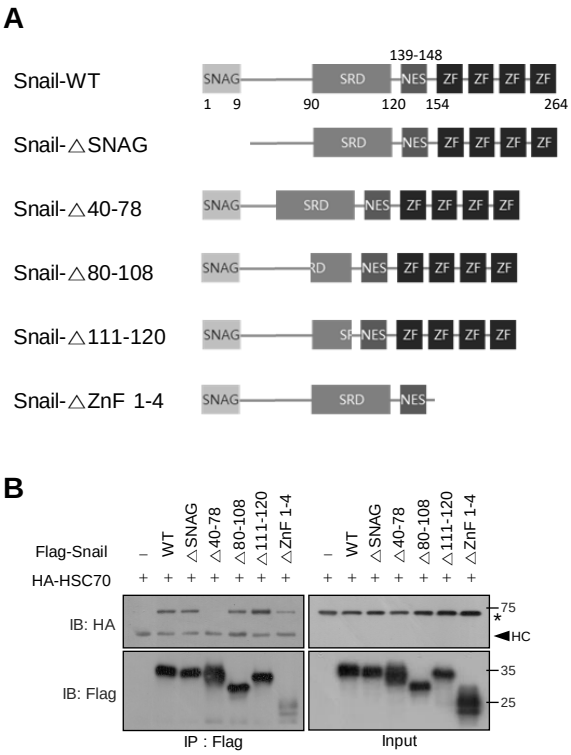

Fig. S2. The amino acid region 40-78 of Snail is essential for its interaction with HSC70. (**A**) Schematic diagram for Snail deletion mutants. (**B**) Interaction between exogenous HSC70 and Snail deletion mutants. HEK293T cells transfected with HA-HSC70 and Flag-tagged respective Snail deletion mutants were immunoprecipitation with anti-Flag antibody and analyzed by western blot using anti-HA antibody.

Supplementary Figure S3

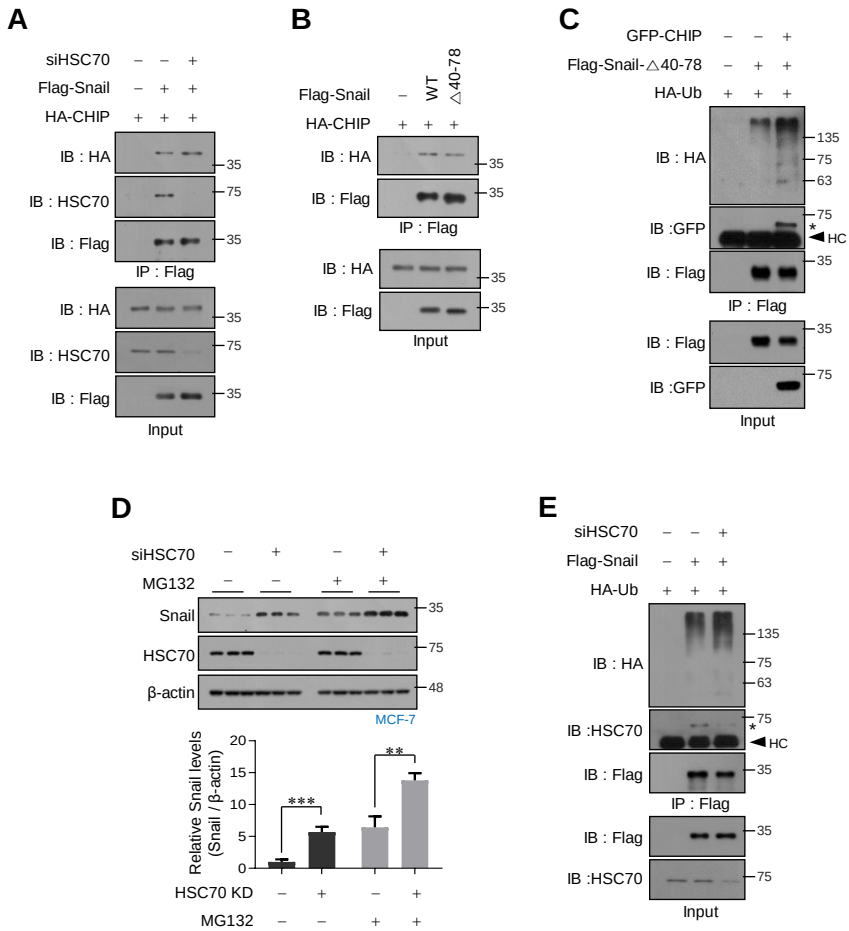

Fig. S3. HSC70 can regulate Snail protein stability independently of proteasome-mediated degradation by CHIP. (**A**) Interaction between exogenous CHIP and Snail in the absence of HSC70. HEK293T cells transfected with HA-CHIP and Flag-Snail were depleted of HSC70. Cell lysates were immunoprecipitated with an anti-Flag antibody and analyzed by western blot using anti-HA antibody. (**B**) Interaction of CHIP with wild-type Snail or Snail-Δ40-78 mutant. HA-CHIP was co-transfected with Flag-tagged wild-type Snail or Snail-Δ40-78 mutant into HEK293T cells. Cell lysates were immunoprecipitated with an anti-Flag antibody and analyzed by western blot using anti-HA antibody. (**C**) HEK293T cells transfected with GFP-CHIP, Flag-Snail-Δ40-78, and HA-ubiquitin were treated with MG132. Cell lysates were immunoprecipitated using anti-Flag antibody and analyzed by western blot using anti-HA antibody. (**D**) HSC70-depleted HEK293T cells were treated with MG132. Cell lysates were immunoblotted with the indicated antibodies (upper). Relative Snail levels were quantified using ImageJ (lower). **, $P < 0.01$: ***, $P < 0.001$ as determined by t-test. (**E**) HSC70-depleted HEK293T cells transfected with Flag-Snail and HA-ubiquitin were treated with MG132. Cell lysates were immunoprecipitated with an anti-Flag antibody and analyzed by immunoblot using anti-HA antibody.

Supplementary Figure S4

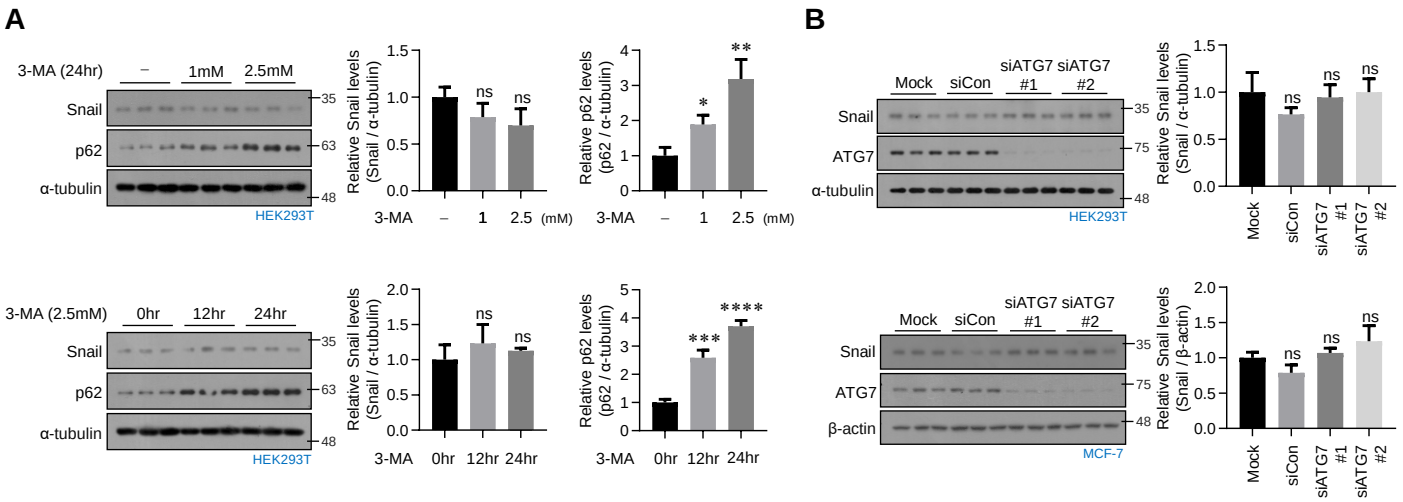

Fig. S4. Macroautophagy does not contribute to Snail degradation. (**A**) Immunoblot analysis in 3-MA-treated HEK293T cells (left). Relative Snail and p62 levels were quantified using ImageJ (right). *, $P < 0.05$: **, $P < 0.01$: ***, $P < 0.001$: ****, $P < 0.0001$ as determined by t-test. ns, not significant. (**B**) Immunoblot analysis in ATG7-depleted HEK293T or MCF-7 cells (left). Relative Snail levels were quantified using ImageJ (right). ns, not significant.

Supplementary Figure S5

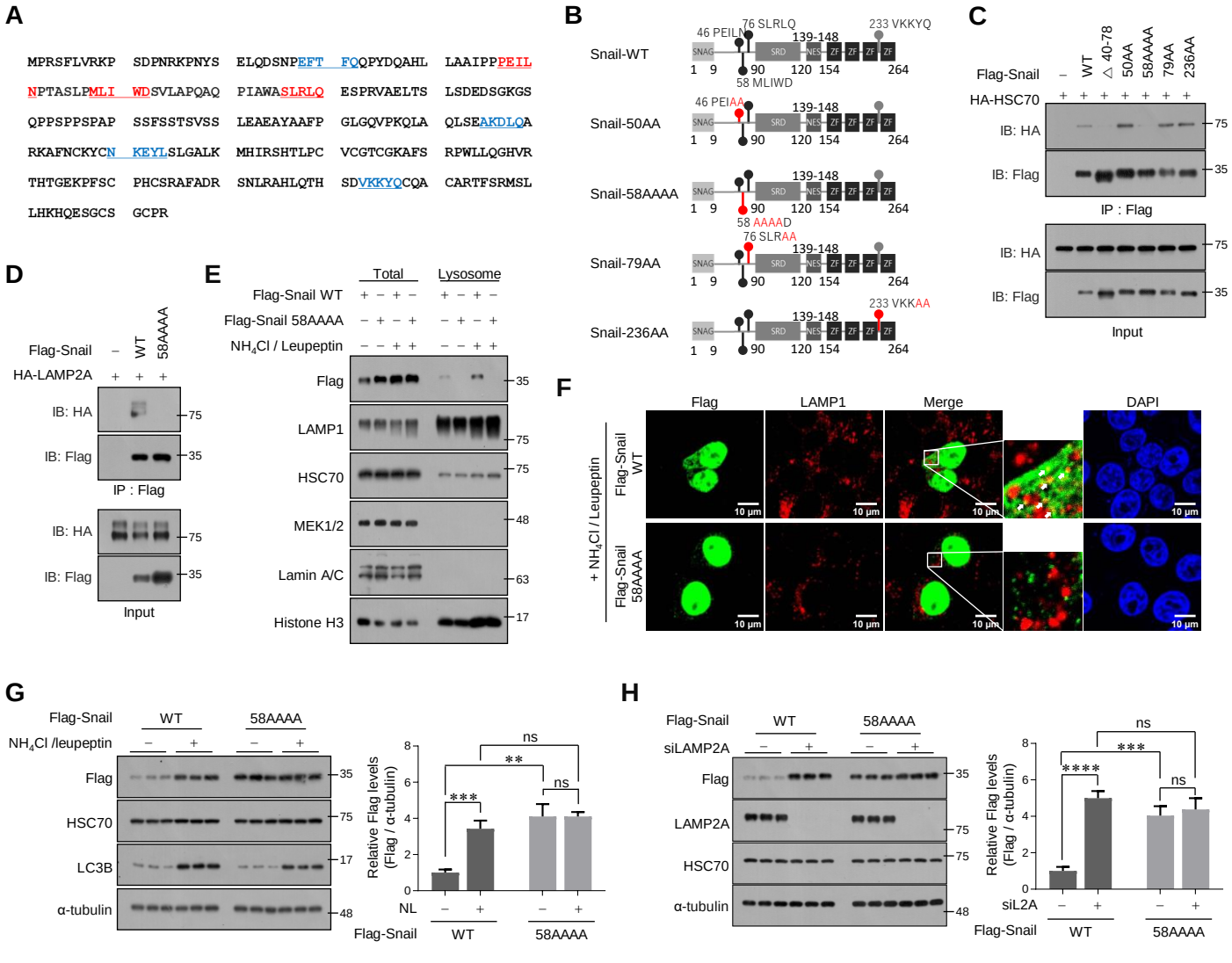

Fig. S5. The 58-62 amino acids region of the Snail protein is a putative recognition motif for CMA. (**A**) KFERQ-like motifs in Snail protein. KFERQ-like motifs within 40-78 amino acids are shown in red, other motifs are shown in blue. (**B**) Schematic diagram for Snail mutants. (**C**) Interaction between exogenous HSC70 and Snail mutants. HEK293T cells transfected with HA-HSC70 and Flag-tagged respective Snail mutants were immunoprecipitation with anti-Flag antibody and analyzed by western blot using anti-HA antibody. (**D**) Interaction of exogenous LAMP2A with WT-Snail or 58AAAA-Snail. HA-LAMP2A was co-transfected with Flag-tagged WT-Snail or 58AAAA-Snail into HEK293T cells. Cell lysates were immunoprecipitated with an anti-Flag antibody and analyzed by western blot using anti-HA antibody. (**E**) WT-Snail accumulation in lysosomes. HEK293T cells transfected with WT-Snail or 58AAAA-Snail were treated with NL. Lysosome lysates were immunoblotted with indicated antibodies. (**F**) Colocalization of WT-Snail with LAMP1. HEK293T cells transfected with WT-Snail or 58AAAA-Snail were treated with NL, and visualized by confocal microscopy after immunostaining with the indicated antibodies. Scale bars, 10 μm. (**G**) Immunoblot analysis of NL-treated WT-Snail- or 58AAAA-Snail-expressing HEK293T cells (left). Relative Snail levels were quantified using ImageJ (right). **, $P < 0.01$: ***, $P < 0.001$ as determined by t-test. ns, not significant. (**H**) Immunoblot analysis in LAMP2A-depleted WT-Snail- or 58AAAA-Snail-expressing HEK293T cells (left). Relative Snail levels were quantified using ImageJ (right). ***, $P < 0.001$: ****, $P < 0.0001$ as determined by t-test. ns, not significant.

Supplementary Figure S6

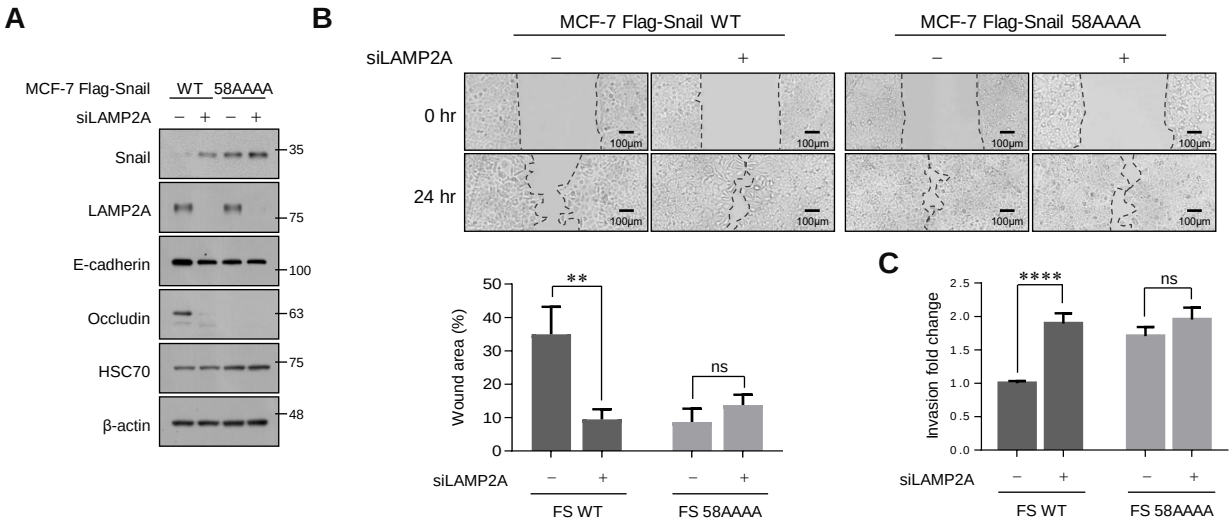

Fig. S6. Effect of LAMP2A depletion in WT-Snail or 58AAAA-Snail-expressing MCF-7 cells on their ability to induce EMT and invasiveness. (**A**) Expression levels of E-cadherin and Occludin in LAMP2A-depleted-WT-Snail or 58AAAA-Snail-expressing MCF-7 cells were analyzed by immunoblotting. (**B**) LAMP2A-depleted-WT-Snail or 58AAAA-Snail-expressing MCF-7 cells were analyzed in wound-healing assays by visualizing wound closure via phase-contrast microcopy (upper). Wound areas were measured using WimScratch software (Wimasis). The data shown represent the percentage of the wound area and are expressed as the means ± SD of three individual experiments (lower). **, $P < 0.01$ as determined by t-test. (**C**) LAMP2A-depleted-WT-Snail or 58AAAA-Snail-expressing MCF-7 cells were seeded onto Matrigel matrix-coated top chambers, and the fold-changes of invading cells were measured after 30 hours. The data shown are expressed as the means ± SD of three individual experiments, each performed in triplicate. ****, $P < 0.0001$ as determined by t-test.

Supplementary Figure S7

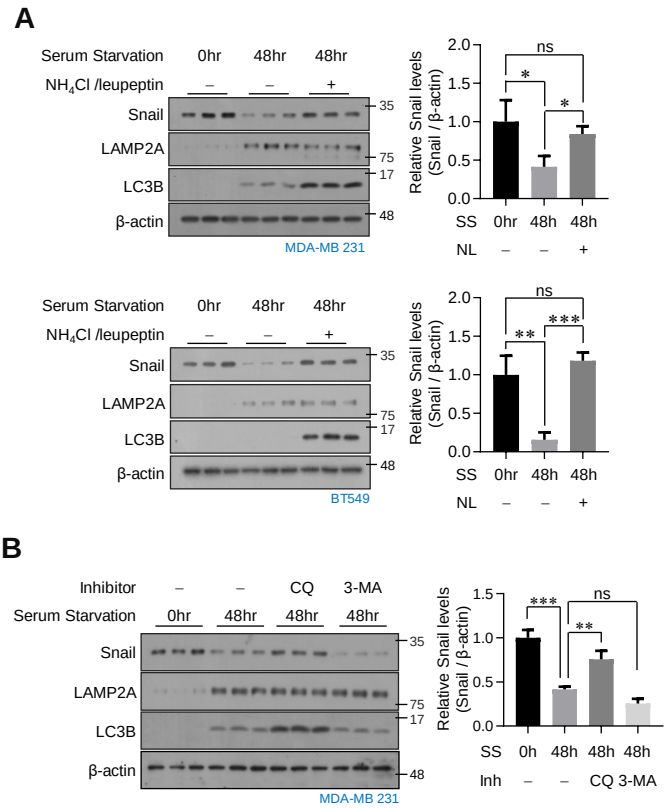

Fig. S7. NL or CQ treatment, but not 3-MA, inhibits serum starvation-induced decrease in Snail expression in TNBC cells. (**A**) Immunoblot analysis of serum-starved MDA-MB-231 or BT549 cells treated with or without NL (left). Relative Snail levels were quantified using ImageJ (right). *, $P < 0.05$: **, $P < 0.01$: ***, $P < 0.001$ as determined by t-test. ns, not significant. (**B**) Immunoblot analysis of serum-starved MDA-MB-231 cells treated with CQ or 3-MA (left). Relative Snail levels were quantified using ImageJ (right). **, $P < 0.01$: ***, $P < 0.001$ as determined by t-test. ns, not significant.

Supplementary Figure S8

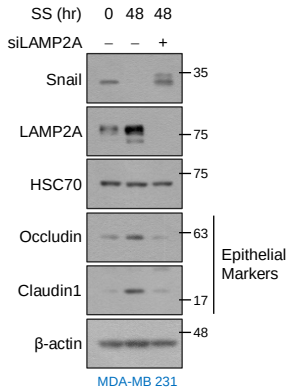

Fig. S8. LAMP2A depletion inhibits serum starvation-induced increase in expression of epithelial marker proteins in MDA-MB-231 cells. Expression levels of epithelial marker proteins in serum-starved MDA-MB-231 cells with or without inhibited expression of LAMP2A were analyzed by immunoblotting.

Supplementary Figure S9

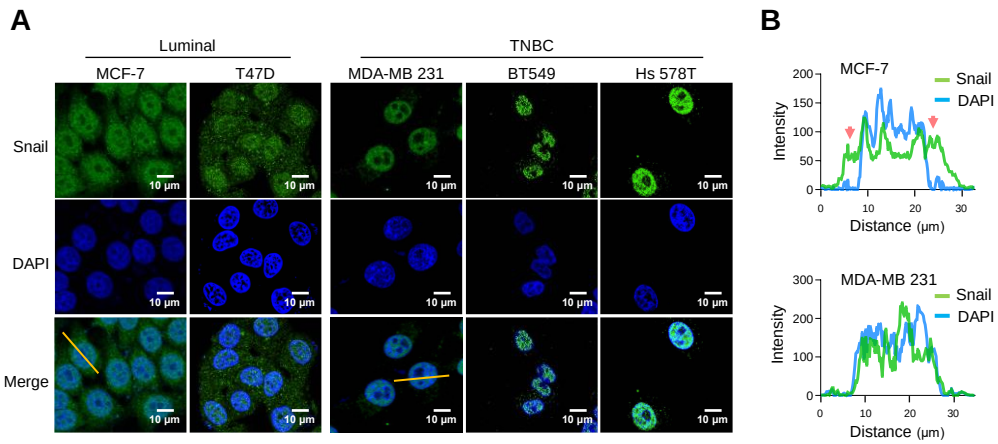

Fig. S9. Subcellular localization of endogenous Snail protein in luminal-type breast cancer cells or TNBC cells. (**A**) Luminal-type breast cancer cells or TNBC cells were visualized by confocal microscopy after immunostaining with the indicated antibodies. Scale bars, 10 μm**.** (**B**) The intensity profiles of the fluorescence signals along the yellow lines indicated in the merge images in (**A**).

Supplementary Figure S10

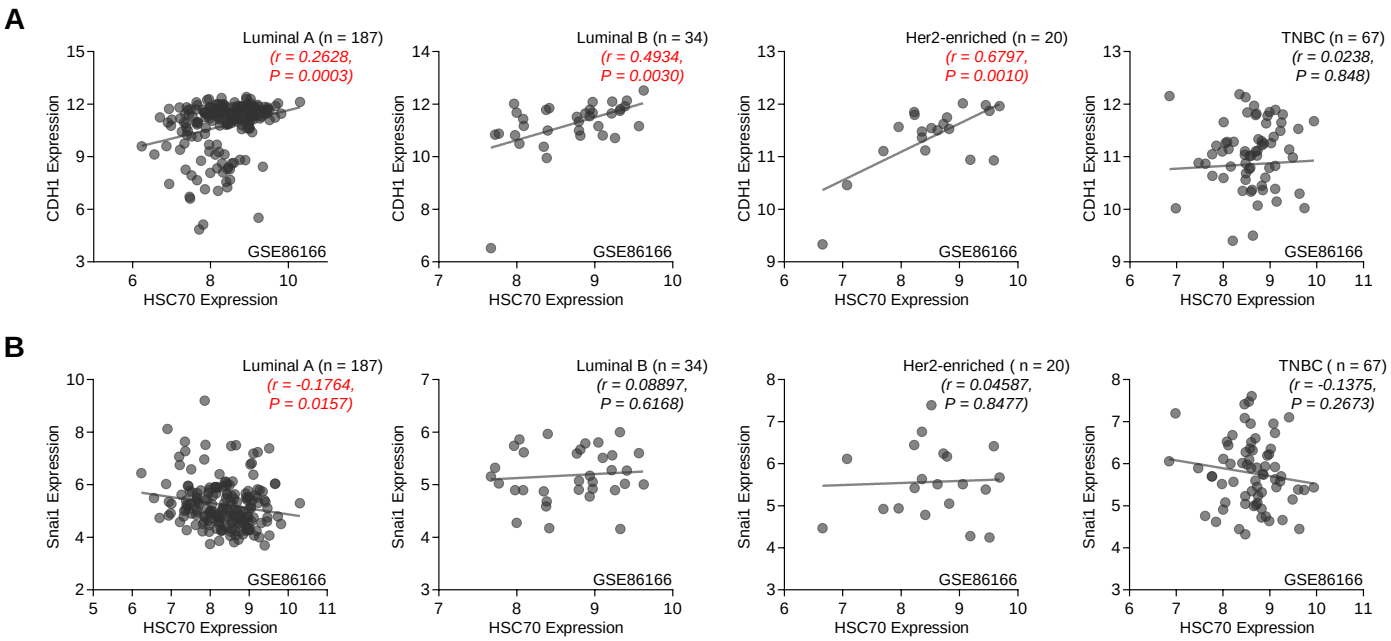

Fig. S10. Expression of HSC70 positively correlates with the expression of E-cadherin in patients with luminal-type breast cancer. (**A**) Correlation of HSC70 expression with E-cadherin (CDH1) expression in breast cancer patients (GSE86166, luminal A-type breast cancer patients, n = 187; luminal B-type breast cancer patients, n = 34; Her2-enriched breast cancer patients, n = 20; TNBC patients, n = 67). (**B**) Correlation of HSC70 expression with Snail expression in breast cancer patients (GSE86166, luminal A-type breast cancer patients, n = 187; luminal B-type breast cancer patients, n = 34; Her2-enriched breast cancer patients, n = 20; TNBC patients, n = 67).